



This is a repository copy of *Silicon oxycarbide glass for the immobilisation of irradiated graphite waste*.

White Rose Research Online URL for this paper:
<http://eprints.whiterose.ac.uk/95392/>

Version: Accepted Version

Article:

Lloyd, J.W., Stennett, M.C. and Hand, R.J. (2016) Silicon oxycarbide glass for the immobilisation of irradiated graphite waste. *Journal of Nuclear Materials*, 469. pp. 51-56. ISSN 0022-3115

<https://doi.org/10.1016/j.jnucmat.2015.11.034>

Reuse

Unless indicated otherwise, fulltext items are protected by copyright with all rights reserved. The copyright exception in section 29 of the Copyright, Designs and Patents Act 1988 allows the making of a single copy solely for the purpose of non-commercial research or private study within the limits of fair dealing. The publisher or other rights-holder may allow further reproduction and re-use of this version - refer to the White Rose Research Online record for this item. Where records identify the publisher as the copyright holder, users can verify any specific terms of use on the publisher's website.

Takedown

If you consider content in White Rose Research Online to be in breach of UK law, please notify us by emailing eprints@whiterose.ac.uk including the URL of the record and the reason for the withdrawal request.



eprints@whiterose.ac.uk
<https://eprints.whiterose.ac.uk/>

Silicon Oxycarbide Glass for the Immobilisation of Irradiated Graphite Waste

James W Lloyd, Martin C Stennett, Russell J Hand*

Immobilisation Science Laboratory, Department of Materials Science and Engineering, Sir Robert Hadfield Building, University of Sheffield, Sheffield, S1 3JD, UK

r.hand@sheffield.ac.uk

Abstract

Silicon oxycarbide glass has been investigated as a potential immobilisation medium for irradiated graphite waste from nuclear power generation. The glass was synthesised via sol-gel techniques using alkoxysilane precursors. Attempts to produce a wasteform via conventional sintering were unsuccessful, but dense wasteforms were achieved by spark plasma sintering (SPS). Microstructural investigations showed that the addition of graphite to the glass did not alter the structure of the matrix; no reaction between the graphite and the glass matrix was observed. Silicon oxycarbide glass is a viable candidate for encapsulation of graphite waste prior to disposal.

1. Introduction

Globally, there are approximately 250,000 tonnes of irradiated graphite that require disposal [1], which is mostly the product of nuclear reactor decommissioning. In many older reactor designs *e.g.* UK's Magnox and Russia's light water graphite moderated reactors (LWGR), graphite was used as a neutron moderator and was present in the core. The now irradiated graphite contains a number of radio-isotopes that are of potential concern [2]:

- Short-lived ^3H , which has a half-life of 12 years. As a result ^3H is of minimal concern for long-term disposition, however as a β -emitter ^3H emission during any graphite treatment processes could be of concern.
- Long-lived ^{36}Cl ; although ^{36}Cl is only present at low levels it has a half-life of over 300,000 years and is readily absorbed by the body.
- Long-lived ^{14}C is the major radio-isotope present in the graphite; mainly generated from nitrogen impurities and neutron capture, and with a half-life of 5730 years, it is a dangerous β -emitter that can be easily ingested as $^{14}\text{CO}_2$.
- It is also possible that the graphite may be contaminated by particulate fuel matter from the reactor core.

Due to its layered structure, graphite irradiated at low temperatures is also able to contain the energy transferred to it by neutron bombardment. This is known as Wigner energy and can cause the graphite to spontaneously self-heat if reheated to temperatures 50 °C above the original irradiation temperature, resulting in handling and fire risks [3]. Therefore it is important that this waste graphite be processed and disposed of safely.

The current recommended method of graphite disposal proposed by the Nuclear Decommissioning Agency (NDA) in the UK is to dispose of it directly in a geological disposal facility (GDF) with additional shielding materials [4]. The main drawback to this method is the large volume of space it will take up in a GDF, where space will be at a premium, and therefore may be prohibitively expensive. Incineration has also been considered, however this will release $^{14}\text{CO}_2$ into the lower atmosphere and although the amount of ^{14}C released to air would be relatively low compared to the amounts generated in the upper atmosphere by natural processes, it is not viewed as a viable solution [5].

As well as the existing irradiated graphite stock some fourth generation (Gen IV) nuclear reactor proposals, namely the very high temperature reactor (VHTR) and pebble bed modular reactor (PBMR), have been designed to use carbonaceous tri-structural isotropic (TRISO) fuel. TRISO fuel particles have been designed for once-through use in an open fuel cycle to deter nuclear proliferation. They consist of a uranium oxide fuel core surrounded by alternating layers of pyrolytic carbon and silicon carbide intended to retain the spent fuel and fission products in a non-easily reprocessable form. The outer pyrolytic carbon layer is graphitic in nature and a robust disposal route must be found for this eventually spent fuel waste [6, 7]. Direct disposal will not be an option and an incorporation or encapsulation system will need to be in place, similar in intent to that currently used for unrecyclable fission products, minor actinides and transuranics.

A number of solutions to the problem of what to do with irradiated graphite have been postulated, but currently none have been optimised. Conventional vitrification is not possible with this waste because the graphite will, at least partially, volatilise in the presence of oxygen at the likely vitrification temperatures [1, 3, 4, 5, 8]. Generally, encapsulation in a cement matrix has resulted in phase separation, and encapsulation in a glass matrix has resulted in porous, structurally weak wasteforms [4], although it has also been suggested that the open pores on the surface of the graphite could be impregnated by a glass under pressure. A number of other conditioning techniques that have been or are being considered for the treatment of irradiated graphite, including epoxy impregnation and the use of geopolymers are outlined by Ojovan and Wickham [9].

Silicon oxycarbides are a family of glasses that already contain carbon, albeit directly bonded to the silicon as a result of the synthesis process. The modelling of Kroll also suggests that the so-called “free” carbon that is found in many silicon oxycarbide glasses is directly bonded to the surrounding silicon oxycarbide matrix [10]. However, they possess many qualities that would be desirable in a wasteform namely physical properties that rival those of vitreous silica and good chemical durability. There has been a reasonable amount of investigation into silicon oxycarbide glasses since their discovery as ‘black glasses’ by Chi in 1983 [11] and a range of applications have identified in electroceramics, coatings, strong glass fibres and thin films [12, 13, 14]. Although the processing atmosphere has to be carefully controlled for oxycarbide glass production the possibility of bonding the graphitic carbon directly into the glassy matrix means that these glasses are potentially attractive for the immobilisation of irradiated graphite. The aim of the work described here was therefore to see if silicon oxycarbide glasses are suitable for use as a matrix for the immobilisation of irradiated graphite waste.

2. Experimental

Synthesis of silicon oxycarbide glass

This synthesis was adapted from that described by Pantano *et al.* [15]. Two equivalents (eq) of triethoxysilane (TREOS, Fluorochem), 1 eq of methyltrimethoxysilane (MTMOS, Fluorochem), and 4 eq of ethanol as a solvent were added to a Teflon reaction vessel. The reaction mixture was stirred to achieve homogenisation. With continued stirring, 5 eq of deionised water were added, before being acidified to pH2 using 0.05 eq of hydrochloric acid (1M) to initiate the hydrolysis. The reaction was stirred at room temperature for 30 minutes. After this, 4 eq of ammonium hydroxide (0.005M) were added drop-wise with stirring to speed up condensation of the polymer. The reaction mixture was then placed in an oven at 60 °C overnight to gel and dry. The resulting polymer was retrieved as a colourless, translucent ‘frit’, with each particle having a diameter of approximately 2 mm. The polymer frit was placed in a tube furnace, flushed with argon, then heated at 3 °C/min to 900 °C where it was held for 1 hour under continuous flowing argon, before being cooled at the same rate to room temperature. The resulting silicon oxycarbide glass was obtained as an opaque black/brown frit.

A number of routes to incorporate graphite in the oxycarbide glass were investigated. Initially graphite was mixed with the polymer gel at the ‘wet chemistry’ stage however dispersal was an issue as the graphite agglomerated at the base of the vessel. A potential solution to this involved adding a surfactant, however this would have introduced additional components prior to pyrolysis

which was deemed undesirable. Graphite was also added to powdered polymer, after gelation was complete. Unfortunately, during the uniaxial pressing, it was not possible to create a green body that retained its shape, even after the addition of a binding agent. Ultimately, the most successful approaches involved adding the graphite to the oxycarbide glass powder prior to the sintering treatments detailed below.

Conventional sintering

The silicon oxycarbide glass was placed in a planetary ball mill and powdered until a particle size of $\leq 250 \mu\text{m}$ was obtained. Pellets were then formed using a uniaxial die and pneumatic press resulting in a green body 13 mm in diameter. The pellets were placed in a tube furnace, which was flushed with argon, then heated at $3 \text{ }^\circ\text{C}/\text{min}$ to $1450 \text{ }^\circ\text{C}$ where it was held for 5 hours under continuous flowing argon, before being cooled at the same rate to room temperature. This process yielded a brittle and deformed opaque black wasteform.

Spark plasma sintering (SPS) of glass/graphite wasteforms

The silicon oxycarbide glass was placed in a planetary ball mill and powdered to a particle size of $\leq 250 \mu\text{m}$. 10, 20 or 30 wt% graphite powder were added and intimately mixed using a pestle and mortar. A sample was also prepared with no graphite addition. Each mixture was then placed in a graphite die lined with graphite foil, then placed in an SPS furnace (FCT Systeme GmbH - Spark Plasma Sintering type HP D 25) which was evacuated then flushed with argon. The die was pressed to 5 kN and heated at $50 \text{ }^\circ\text{C}/\text{min}$ to $550 \text{ }^\circ\text{C}$. The pressure was increased to 11 kN and the sample heated at $100 \text{ }^\circ\text{C}/\text{min}$ to $1300 \text{ }^\circ\text{C}$ where it was held for 20 minutes in an argon atmosphere. The sample was cooled at $100 \text{ }^\circ\text{C}/\text{min}$ to room temperature and the pressure released. After removal of the graphite foil, this process yielded wasteforms 20 mm in diameter: opaque black (0 wt% added graphite), or opaque with grey particulate graphite (10, 20, 30 wt% added graphite).

Fourier Transform Infrared (FTIR) spectroscopy of the silicon oxycarbide glass and glass-graphite composites was conducted using a Perkin Elmer Frontier FTIR operating in Attenuated Total Reflectance (ATR) mode. Prior to measurement the sample was ground to a powder in a pestle and mortar and the powder was placed on the ATR anvil and compressed. A 4-scan background was taken before each sample was run and each sample was scanned 16 times. X-ray powder diffraction was undertaken using a Siemens D5000 diffractometer with $\text{CuK}\alpha$ ($\lambda = 1.54056 \text{ \AA}$) radiation operating between 10 to $70 \text{ }^\circ 2\theta$ with a step size of $0.05 \text{ }^\circ 2\theta$.

For microstructural investigations the cylindrical samples were cut across their diameter and then cold-mounted in epoxy resin. The mounted samples were successively ground using 240-1200 SiC grit paper before polishing on a cashmere cloth coated with progressively finer (6 down to 1 μm) diamond suspensions. Water was the lubricant for all stages. Optical microscopy was undertaken using a Nikon Labophot 2 typically at 5 \times to 50 \times magnification. Scanning electron microscopy (SEM) was conducted with a JEOL JSM 6400, using an accelerating voltage of 12 kV, coupled with energy dispersive x-ray spectroscopy (EDX; Oxford Instruments ISIS 300). Prior to SEM inspection the polished sample surfaces were carbon coated.

3. Results and Discussion

The organosilicon reagents used were chosen based on their ability to give a low free-carbon content of $\leq 5\%$ within the silicon oxycarbide glass. It was thought that if more carbon was being added to the matrix, it would be beneficial to begin with the least amount of elemental carbon already present in the glass. According to Babonneau *et al.* [16], if both reagents contain silicon-hydrogen bonds carbothermal reduction is more likely to happen during pyrolysis of the gel, resulting in a higher concentration of silicon-carbon bonds and hydrogen outgassing.

The pyrolysed polymer gel was found to be x-ray amorphous suggesting that a glass had been formed (Fig 1, green line). FTIR spectroscopy showed that the transition from polymer to glass was successful. It can be seen in Fig 2 that bands representative of C-H (2981 cm^{-1}) and Si-H (1264 cm^{-1} , 2186 cm^{-1} , 2249 cm^{-1}) bonds diminish in height. The two bands indicating the presence of Si-CH₃ (825 cm^{-1} , 765 cm^{-1}) coalesce and diminish also, and a broad band indicative of undefined Si-C bonding, as opposed to the distinct Si-C-H bonding bands, appears. This shows that the carbothermal reduction necessary for Si-C-Si formation has occurred with the Si-C and Si-H bonds being broken. The Si-O-Si band has also broadened and shifted slightly, again indicating that the bonding has become less defined and more complex as more Si-C bonds are formed. The resulting picture is that of a silicon oxide glass matrix where a proportion of the silicon is bonded through bridging carbon atoms, as opposed to bridging oxygen atoms; *i.e.* a silicon oxycarbide glass. Attempts to measure T_g by DTA were unsuccessful; as pointed out by Pantano *et al* [15] T_g can be expected to be greater than the pyrolysis temperature but exceeding this temperature during the measurement will lead to further structural changes and thus changes to the property you are trying to measure.

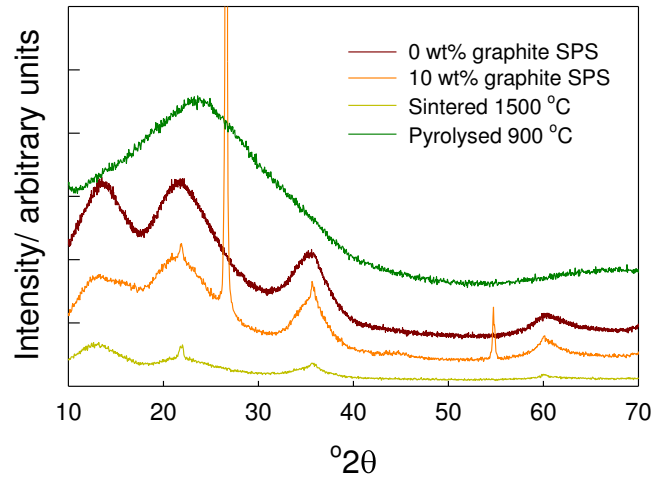


Figure 1 Powder x-ray diffraction patterns showing how the crystallisation behaviour changes with processing conditions.

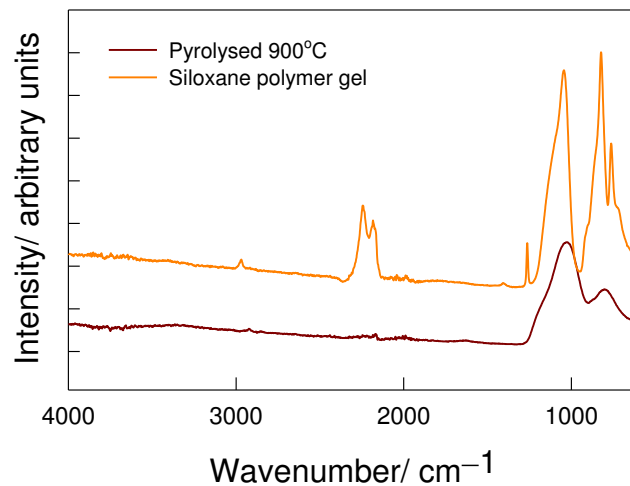


Figure 2 FTIR spectra showing the differences between the polymer gel and silicon oxycarbide glass.

The as prepared glass was then pulverised, pressed and the green body was sintered in a tube furnace at 1500 °C for 5 hours to assess whether a suitable wasteform could be produced via a simple cold press and sinter route. The products obtained were warped, deformed and very brittle, to the extent that they fell apart when handled. The diffraction pattern for this sample showed three broad bands with reduced intensity (Fig 1, mustard yellow line), although the overall amorphous character of the trace was retained. At the very centre of each band a small sharp reflection is visible indicating the onset of crystallisation: the 21.7 $^{\circ}2\theta$ reflection is probably due to the (101) cristobalite plane and the 34.9 and 60.0 $^{\circ}2\theta$ reflections are probably due to the (111) and (220) planes of β -silicon carbide, although a definitive identification could not be made. Despite silicon oxycarbide

glasses showing resistance to devitrification [17], they have also proven difficult to sinter [11]; in this case the high temperatures and holding times necessary to achieve a sintered body are likely to be the cause of the crystallisation and deformation. The FTIR spectrum for this glass shows the appearance of a shoulder and small band (809 cm^{-1}) in the Si-C bonding region (Fig 3, green solid line). The small band indicates that there is significant Si-C bonding; this correlates with the onset of crystallisation of β -silicon carbide identified by XRD. A shoulder also develops to the left of the Si-O-Si band (1229 cm^{-1}) implying more silicon is becoming bonded to carbon. Due to the poor physical properties of the product, a different processing technique for sintering the glass was sought. No attempt to combine the glass with the graphite was made using conventional sintering.

Spark plasma sintering (SPS) relies on pulsing a DC current through a graphite die resulting in internal Joule heating of the sample. This allows for high heating and cooling rates when compared to conventional heating, and a reduction in residence time within the furnace. In addition, a pressure can be applied throughout the heating and cooling cycle yielding samples that almost achieve theoretical density. SPS was selected as an alternative processing method, enabling the holding time to be reduced to 30 minutes, with heating and cooling rates of the order of $100\text{ }^{\circ}\text{C}/\text{min}$. The applied pressure allowed for samples of over 97% theoretical density to be obtained. The diffraction pattern for the resulting oxycarbide glass (Fig 1, red line) showed the same overall shape as the conventionally sintered glass. It is thought that the observed regions of diffuse intensity are representative of nanocrystalline regions within the glass matrix where there is insufficient long-range order to show up as well defined reflections in the diffraction pattern. The crystallisation indicated by the small reflections in the centre of each region of diffuse intensity, seen in the conventionally sintered sample, were not observed. This suggests that the long heating cycle and residence time during conventional sintering are responsible for crystal growth. The FTIR analysis of this glass was also similar, again showing the development of a shoulder at 890 cm^{-1} , and 1229 cm^{-1} indicating increased silicon-carbon bonding. Interestingly, the small, sharper band at 809 cm^{-1} was absent, indicating that no crystallisation has occurred in these samples.

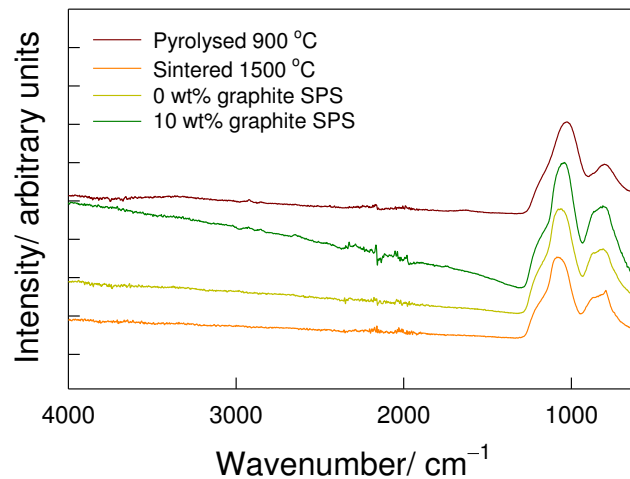


Figure 3 FTIR spectrum showing the similarities in bonding obtained using different processing methods, and with the addition of graphite.

The addition of the graphite to the glass before sintering yielded similar results to samples containing only glass. There were two new intense peaks present due to the graphite (002) and (004) reflections at 26.4° , 54.7° 2θ (Fig 1, orange line). The presence of the graphite also resulted in the return of the small peaks that are likely silicon carbide and cristobalite reflections. This can be explained by the graphite acting as a heterogeneous nucleating agent. The FTIR data (Fig 2, green) showed no change in chemical bonding. This leads to the question as to whether the graphite reacts with the glass matrix at all. The intense graphite reflections in the XRD pattern imply that either the graphite has not interacted with the glass, therefore not becoming incorporated within the matrix; or there has been a surface interaction, but the graphite particles are too large to become fully incorporated. The latter case is similar to the graphite acting as bonded “free” carbon in the glass matrix.

Optical microscopy showed that the microstructures of the glass-graphite composites formed through spark plasma sintering contained no visible porosity at loadings of either 10 or 20 wt% graphite (Fig 4). The graphite was present as discrete regions within the glass matrix, clearly indicating that the graphite had not fully reacted with the glass matrix, although closer inspection shows that there is good contact between the glass and the graphite (Fig 5). It is believed that this is due to the use of an inert atmosphere during processing, which avoids oxidation and the build-up of trapped carbon dioxide gas around the graphite. It was noted that at higher waste loadings, the volume of graphite became larger than that of the glass. In these cases, the wasteform can be more accurately described as ‘glass in a graphite matrix’, rather than ‘graphite in a glass matrix’. Similar observations were made by McGann and Ojovan [18].

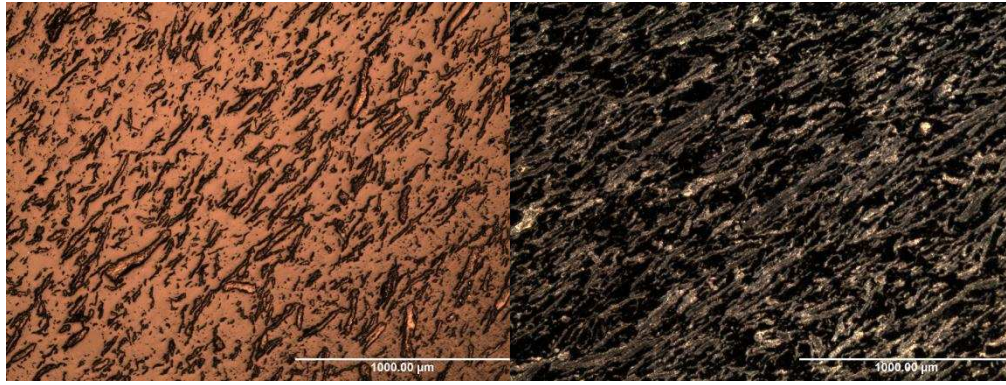


Figure 4 Optical micrographs showing absence of visible porosity: a) Bright field image of glass-graphite composite (10 wt%, SPS); b) dark field image of glass graphite composite (20 wt%, SPS), black represents glass.

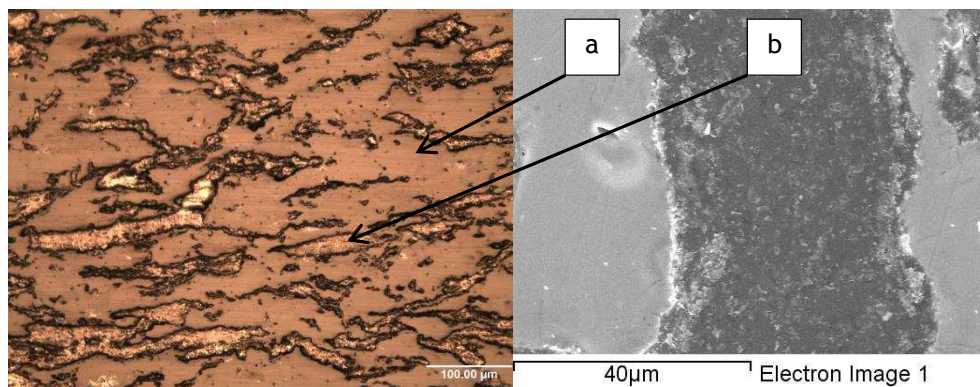


Figure 5 Images (20 wt.%, SPS) showing good contact between the glass and the graphite, a: glass; b: graphite.

The contact between the glass and the graphite was further investigated using EDX spectroscopy to see if there was any evidence of chemical bonding. The steep gradient and ‘top-hat’ shape of the EDX line spectra at the interface between the glass and the graphite strongly suggests that there is no significant interaction: no silicon has diffused into the graphite (Fig 6). A shallower gradient would imply that there had been diffusion between the two and therefore an interaction. Hence, it is likely that any silicon carbide visible in the XRD pattern results solely from high-temperature processing of the glass, with the graphite acting as an inert nucleating agent rather than any graphite reacting to form silicon carbide. It should be noted that the lack of obvious chemical interaction does not mean that there are no bonds between the “free” graphite and the glass.

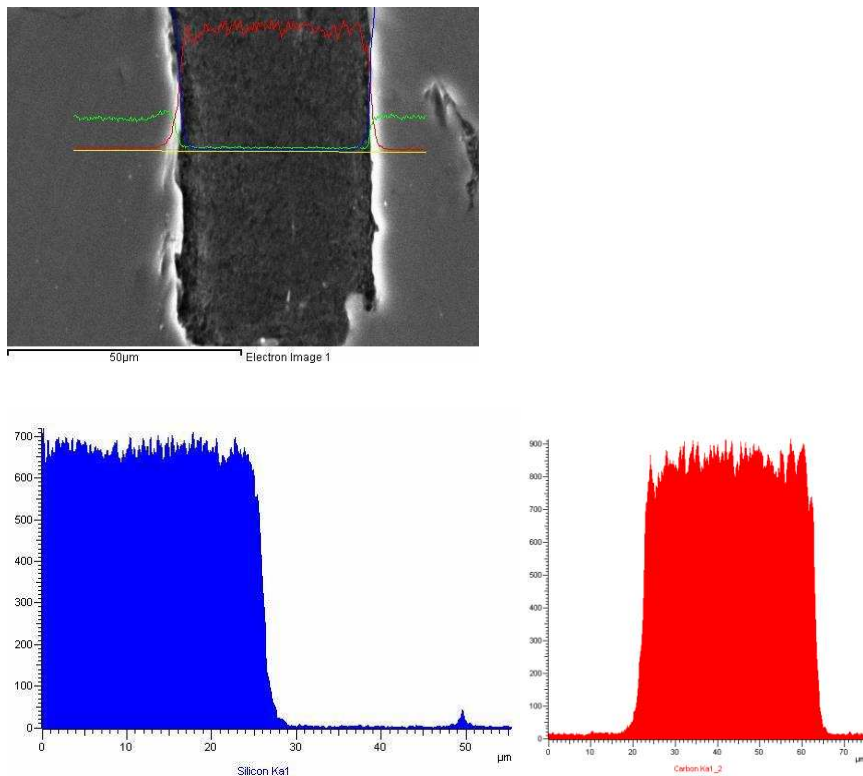


Figure 6 EDX line spectra across a glass-graphite boundary (10 wt.%, SPS). a) SEM image showing the line cross-section; b) data for silica; c) data for carbon.

Although complete chemical incorporation of the graphite was the goal, the excellent physical properties of silicon oxycarbide glass [15] and good contact between glass and graphite mean that this glass could still be a viable host for encapsulation of irradiated graphite. The use of spark plasma sintering as a processing method also enabled the production of a high density wastefrom; less than 3% porosity compares favourably with the literature [17, 19] which would potentially increase the mechanical durability.

As there is no apparent interaction between the glass and the graphite and thus no need to minimise free carbon content within the glass different reagents could be used to create the precursor polymers. This will allow the development of a more economically viable method, for production of the silicon oxycarbide glass wastefroms, on a larger scale.

5. Conclusions

Silicon oxycarbide glass was successfully synthesised and combined with graphite for the first time to create a wastefrom potentially useful for disposal of graphitic waste. Conventional processing of the wastefrom in a tube furnace yielded poor results; brittle samples displaying some crystallisation were produced. Changing the processing method to spark plasma sintering resulted in dense, low porosity samples with vastly reduced holding times and a lower processing temperatures. Good

contact between the glass and graphite was observed in these wasteforms, with no apparent oxidation of the graphite, however there is no apparent large scale chemical incorporation of carbon from the graphite into the glass matrix. Hence oxycarbide glasses may be useful in forming an encapsulant wasteform for irradiated graphite.

Use of the glass as an encapsulant relaxes the criterion for the selection of the polymer precursors required to synthesis the oxycarbide glass. Hence alternative, less costly polymers could be synthesised making it cheaper to produce larger volumes of material. As well as providing potential encapsulant wasteforms for irradiated graphite the compatibility of oxycarbide glasses with TRISO fuel particles should also be investigated as providing a potential stable wasteform for future fuel wastes.

Acknowledgements

JWL would like to thank the E-Futures Doctoral Training Centre, University of Sheffield and the EPSRC for the funding to conduct this research. The authors would also like to thank Mr Ben Palmer, Mr Kyle Arnold and Dr Amit Rana for their help and support throughout this project.

References

1. IAEA, "Characterization, Treatment and Conditioning of Radioactive Graphite from Decommissioning of Nuclear Reactors", IAEA TECDOC 1521, IAEA, Vienna, 2006.
2. Yim M-S. & Caron F., "Life cycle and management of carbon-14 from nuclear power generation", *Progress in Nuclear Energy*, 2006, **48**, 2-36.
3. IAEA, "Management of waste containing tritium and carbon-14", *Technical Reports Series No. 421*, IAEA, Vienna, 2004.
4. NDA, "Geological Disposal: Review of baseline assumptions regarding disposal of core graphite in a geological disposal facility", *NDA Technical Note no. 16495644*, NDA, Didcot, 2012.
5. Electric Power Research Institute (EPRI), "Graphite Decommissioning - Options for Graphite Treatment, Recycling, or Disposal, including a discussion of Safety-Related Issues", *EPRI Technical Report ref: 1013091*, EPRI, Concord, CA, 2006.
6. U.S. DOE (Department of Energy) Nuclear Energy Research Advisory Committee and the Generation IV International Forum, "A Technology Roadmap for Generation IV Nuclear Energy Systems", *U.S. DOE Report GIF-002-00*, 2002.
7. Price M. S. T., "The Dragon Project origins, achievements and legacies", *Nuclear Engineering and Design*, 2012, **251**, 60-68.

8. Karlina O. K., Klimov V.L., Ojovan M.I., Pavlova G.Yu., Dmitriev S.A. & Yurchenko A.Yu., "Immobilization of carbon-14 from reactor graphite waste by use of self-sustaining reaction in the C–Al–TiO₂ system", *Journal of Nuclear Materials*, 2005, **345**, 84-85.
9. Ojovan M. I. and Wickham A. J. "Treatment of irradiated graphite to meet acceptance criteria for waste disposal: problem and solutions", *Mater. Res. Soc. Symp. Proc. Vol. 1665*, 2014, pp3-12.
10. Kroll P. "Modeling the 'free carbon' phase in amorphous silicon oxycarbide", *J. Non-Cryst. Solids*, 2005, **351**, 1121-1126.
11. Chi F. K., "Carbon-containing monolithic glasses via the sol-gel process", *Ceram. Eng. Sci. Proc.*, 1983, **4**, 704–717.
12. Yang Y., Peng W-J., Guo H-J., Wang Z-X., Li X-H., Zhou Y-Y. & Liu Y-J, "Effects of modification on performance of natural graphite coated by SiO₂ for anode of lithium ion batteries", *Trans. Nonferrous Metal. Soc. China*, 2007, **17**, 1339-1342.
13. Suyal N., Krajewski T. & Mennig M., "Sol-Gel Synthesis and Microstructural Characterization of Silicon Oxycarbide Glass Sheets with High Fracture Strength and High Modulus", *J. Sol-Gel Sci. Technol*, 1998, **13**, 995-999.
14. Wolfe D.M., Hinds B.J., Wang F., Lucovsky G., Ward B.L., Xu M., Nemanich R.J., & Maher, D.M. "Thermochemical stability of silicon–oxygen–carbon alloy thin films: A model system for chemical and structural relaxation at SiC–SiO₂ interfaces", *J. Vac. Sci. Technol. A*, 1999, **17**, 2170-2177.
15. Pantano C. G., Singh A. K. & Zhang H., "Silicon Oxycarbide Glasses", *J. Sol-Gel Sci. Technol.*, 1999, **14**, 7-25.
16. Babonneau F., Bois L. & Maquet J., "Structural Characterization of Sol-Gel Derived Oxycarbide Glasses. 2. Study of the Thermal Stability of the Silicon Oxycarbide Phase", *Chem. Mater.*, 1995, **7**, 975-981.
17. Walter S., Soraru G.D., Bréquel H. & Enzo S., "Microstructural and mechanical characterization of sol gel-derived Si–O–C glasses", *J. Europ. Ceram. Soc*, 2002, **22**, 2389-2400.
18. McGann O. J. & Ojovan M. I., "The synthesis of graphite–glass composites intended for the immobilisation of waste irradiated graphite", *Journal of Nuclear Materials*, 2011, **413**, 47-52.
19. Sujith R., Srinivasan N. & Kumar R. "Small-Scale Deformation of Pulsed Electric Current Sintered Silicon Oxycarbide Polymer Derived Ceramics", *Adv. Engng. Mater.*, 2013, **15**, 1040-1045.